

Article

Assessing the Orange Tree Crown Volumes Using Google Maps as a Low-Cost Photogrammetric Alternative

Carmen Marín-Buzón ¹, Antonio Pérez-Romero ¹, Fabio Tucci-Álvarez ¹ and Francisco Manzano-Agugliaro ^{2,*}

¹ Graphic Engineering Department, University of Sevilla, Utrera Road, km 1, 41013 Sevilla, Spain; carmenmarin@us.es (C.M.-B.); tao@us.es (A.P.-R.); fabiotuccialvarez@gmail.com (F.T.-Á.)

² Department of Engineering, CEIA3, University of Almeria, 04120 Almeria, Spain

* Correspondence: fmanzano@ual.es

Received: 20 May 2020; Accepted: 19 June 2020; Published: 23 June 2020



Abstract: The accurate assessment of tree crowns is important for agriculture, for example, to adjust spraying rates, to adjust irrigation rates or even to estimate biomass. Among the available methodologies, there are the traditional methods that estimate with a three-dimensional approximation figure, the HDS (High Definition Survey), or TLS (Terrestrial Laser Scanning) based on LiDAR technology, the aerial photogrammetry that has re-emerged with unmanned aerial vehicles (UAVs), as they are considered low cost. There are situations where either the cost or location does not allow for modern methods and prices such as HDS or the use of UAVs. This study proposes, as an alternative methodology, the evaluation of images extracted from Google Maps (GM) for the calculation of tree crown volume. For this purpose, measurements were taken on orange trees in the south of Spain using the four methods mentioned above to evaluate the suitability, accuracy, and limitations of GM. Using the HDS method as a reference, the photogrammetric method with UAV images has shown an average error of 10%, GM has obtained approximately 50%, while the traditional methods, in our case considering ellipsoids, have obtained 100% error. Therefore, the results with GM are encouraging and open new perspectives for the estimation of tree crown volumes at low cost compared to HDS, and without geographical flight restrictions like those of UAVs.

Keywords: Google maps; photogrammetry; HDS; TLS; LiDAR; tree crown; UAV; orange tree

1. Introduction

Citrus cultivation is worldwide widespread [1]. Among citrus fruits, the cultivation of the orange tree (*Citrus sinensis* (L.) Osbeck) is considered the most important from a commercial point of view and the Mediterranean climate is especially suitable for its cultivation [2]. All crops are challenged by multiple biotic and abiotic stresses [3], and citrus is no exception [4].

Whitney [5] reported that for orange production, soluble solids and net yields were associated with tree canopy volume. Likewise, for irrigation needs calculation of a crop, the well-known expressions that use crop coefficients in relation to reference evapotranspiration (ET₀) are used [6–8]. Among the factors used in adjusting or modelling ET in crops are the leaf area index or tree volumes [9]. When there are different types of crops or sizes of trees, optimization techniques can be used to make more efficient use of water [10]. As an example, accounting for the variability of tree size within a row in irrigation allows the adjustment of discharge rates to individual tree size, and this could result in significant water savings [11]. Reducing irrigation reduces groundwater contamination by e.g., nitrate leaching [12]. In summary, the volume of the orange tree crown is associated with the production and its quality and it is important for the efficient calculation of the irrigation doses.

On the other hand, the specific information about the leaf volume of the fruit trees is an important factor in determining the doses or spray volumes for the protection of the trees. Studies have shown that the precise dosage of pesticides according to tree shape and foliage volume allows for a saving of 30% [9]. Recent research also supports the need to establish procedures for identifying pesticide doses. For this purpose, especially in “three-dimensional” crops, such as vineyards, olive, and citrus plantations [13], the most appropriate amounts of pesticides can be established with the volume of the crown.

The relevance comes from the fact that pesticide dosing procedures are based on parameters such as leaf wall area or tree row volume, i.e., factors related to the structure of the canopy [14]. Then to ensure that the optimal amount of pesticide should be systematically distributed in all leaf areas, for all crop species and under all conditions it would be necessary to know the tree crown volumes [15]. Therefore, the high level of canopy variability has limited the development of global solutions to ensure the effectiveness of the spraying procedure. In summary, accurate tree crown profiling is vital for adjustment of spray doses in the agriculture of the future and can be used as an important basis for monitoring tree growth and estimating tree biomass [16].

Worldwide research on tree crown volume, according to the Scopus database, is led by the USA, followed by China, Canada, France, Japan, Germany, Spain, Finland, Italy, and Australia. The 5 institutions that have done the most research in this field are the United States Department of Agriculture (USDA) Forest Service, Beijing Forestry University, Chinese Academy of Sciences, Canadian Forest Service and Sveriges lantbruksuniversitet.

To get an overview of the research carried out in relation to the tree crown volume and its estimation, an analysis has been made on the Scopus database. The specific search query was: (TITLE-ABS-KEY (“tree crown*”) AND TITLE-ABS-KEY (volume) OR TITLE-ABS-KEY (estimation)). Apart from the search terms, it was obtained that the main keywords of all these publications were, according to the number of appearances: Forestry, Remote Sensing, Optical Radar, Canopy Architecture, Biomass, Image Analysis, and LiDAR. With all these published works, an analysis of clusters or thematic sets is carried out according to the relationship between them. For this purpose, the Vosviewer software is used, and Figure 1 is obtained where 5 clusters or research trends in this field can be seen.

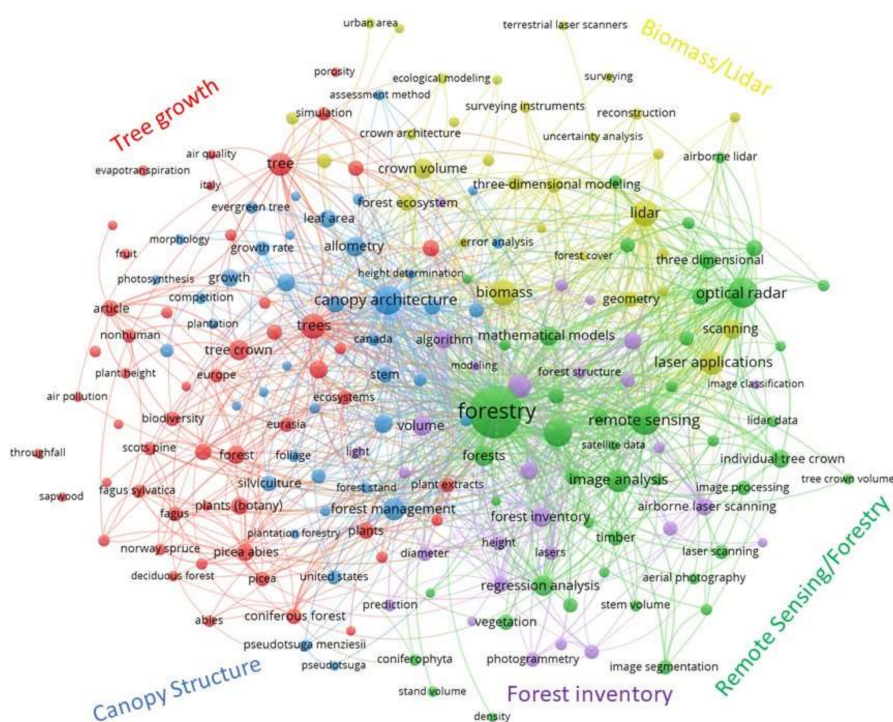


Figure 1. Research trend clusters related to tree crown volume estimation.

The main cluster, in red, is focused on ecosystems and tree growth. Studies related to the forest inventory with LiDAR [17], or the evapotranspiration of European beech trees (*Fagus sylvatica* L.) [18], stand out. The first studies in relation to evapotranspiration were based on geometric ground-based measurements of tree height, height to crown radii. Crown shapes are modelled as solid geometric shapes based on these measures [19]. This last study was for forestry trees, and although cones are useful for modelling conifers, they conclude that paraboloids are versatile shapes that are adaptable to a wide variety of crowns, in this regard ellipsoids are similar to paraboloids for old-growth tree crowns. The main tree types studied are *Pinus* [20,21], *Picea* [22], or *Fagus* [23], *Eucalyptus* [24] and *Quercus* [25,26].

The second cluster, in green, is focused on remote sensing and forestry, as suggested by its main keywords: image analysis [27], Quickbird [28] and airborne lidar data [29]. The third cluster, in blue, is focused on the tree's morphology, where the main keywords are: canopy structure [30,31], forest management [32], deciduous trees [33], allometry, growth, leaf area, and morphology [34]. The fourth cluster, in yellow, is oriented towards biomass and the use of lidar: laser applications, scanning, and geometry data acquisition [35]. Finally, the fifth cluster, in purple, is focused on forest inventory [36]: height, algorithm and diameter.

The manual measurement or traditional method of the crown volume of orange trees is time-consuming and laborious [37], and if it uses many dimensions of these to obtain a better geometry it makes it even more tedious [38]. The traditional methods for assessing tree crown are Vertical Crown Projected Area method (VCPA), Ellipsoid Volume method (VE) and Tree Silhouette Volume method (VTS) [13]. Alternatively, some authors have proposed the use of ultrasonic sensors to measure the volume of the citrus crown due to its easy handling and management and its affordable data processing in real-time [14,39,40].

However, other authors question the accuracy of measurements with this last method [41]. In addition, it has been found that laser technology, LiDAR, achieves higher accuracy compared to ultrasonic sensors [42–44]. These LiDAR techniques have been successfully used on orange plantations even for estimating the harvest and counting oranges [45].

On the other hand, the estimation of the tree crown size is successfully solved by means of aerial photogrammetry, but the cost is too high for orchard trees, such as oranges, when using large airplane flights such as those mentioned above. However, UAV (Unmanned Aerial Vehicles) technology makes it possible to quickly capture significant areas of land at a reasonable time and cost [46]. The use of UAVs has led to the widespread use of aerial photogrammetry in many more fields than was previously available. The techniques we are now using are based on the traditional ones, but the requirements, the necessary equipment and the complexity of the tasks have been reduced considerably. Hence, UAV photogrammetry can be understood as a low-cost photogrammetric measurement tool. This has been used in a lot of situations where it was not possible before, such as archaeological sites [47], or in forestry and agriculture [48].

Thus, the acquisition of massive information has been a permanent feature in the history of the world and photogrammetry has played a part in this. Furthermore, with the digital photography associated with the development of image processing and their automation, these techniques have become widely attractive in diverse areas of implementation. Nowadays the use of online information in our environment is in great demand for all kinds of social applications and is increasingly used for research purposes. Given this, cartography platforms such as Google Earth (GE) are widely used to provide a clear overview of areas or buildings [49], elevation data [50], or enhance geo-tourism using augmented reality [51].

Online platforms for global coverage with aerial information about the territory started to be developed with the Earth Viewer (Keyhole, Inc., Mountain View, California, USA) in 1999 and were extended until the year 2000. On 21 May 2005 Keyhole also a precursor of the KML (Keyhole Markup Language) format [52] was renamed Google Earth (GE). This program was launched on 28 June 2005, having as a main novelty, apart from the change of name and owner, that the program had a free

version [53]. This platform also incorporates Google Maps (GM), giving the functionality to Google Earth as a search engine to find streets, avenues or even businesses and expand them in a very readable way. Thus, under the name of Google Earth, the company of the famous search engine has developed a set of tools that combines aerial photographs, maps, three-dimensional images and information, so that it can simulate a zoom of the entire planet and a travelling of any point any other. This platform (GM) introduced a mapping service that was significantly easier and more user-friendly than the market leaders at the time, such as Multimap.com and Streetmap.co.uk in the UK; Mapquest in the USA; and ViaMichelin in Europe.

Today it can be affirmed that GM has greatly increased user expectations and that its widespread popularity has replaced all other applications. In parallel, Google Street View (GSV) images along user-selected routes can generate environment volumes that can be associated with GM [54]. So, the use of GM is widespread for other types of applications, but especially for two-dimensional uses such as routes or distances [55], or GIS [56]. However, GM's innovative agricultural applications are not yet fully exploited. In the literature, one finds mainly solutions that were developed to get online maps, for example. A case study of developing an online map service to display the locations of hundreds of gardens on the Internet for the United States Department of Agriculture (USDA) [57].

As GM can supply extensive data related to the topography, and land objects of a region due to its undoubted advantages such as wide use, lack of charge and quick update. That is, to generate the geometric properties of the tree crown from the information acquired from several redundant images obtained from GM because with photogrammetric techniques it is possible to generate a three-dimensional model if information from images from different points of view are available. In this study, the aim was to assess its potential use for estimating orange tree crown size, in relation to both traditional and more modern methods mentioned above.

2. Data

The trials conducted in this study were performed on orange trees. The situation of the crop was in Seville in the south of Spain, Figure 2. In particular, the trial was in the field of agricultural practices of the University of Seville, $37^{\circ}21'4.97''$ N, $5^{\circ}56'9.82''$ W, Figure 3. This plot was chosen because it has different crown sizes of orange trees. The 9 trees under study have been marked with a red dot in the zoom of Figure 2.



Figure 2. Location of the trials.

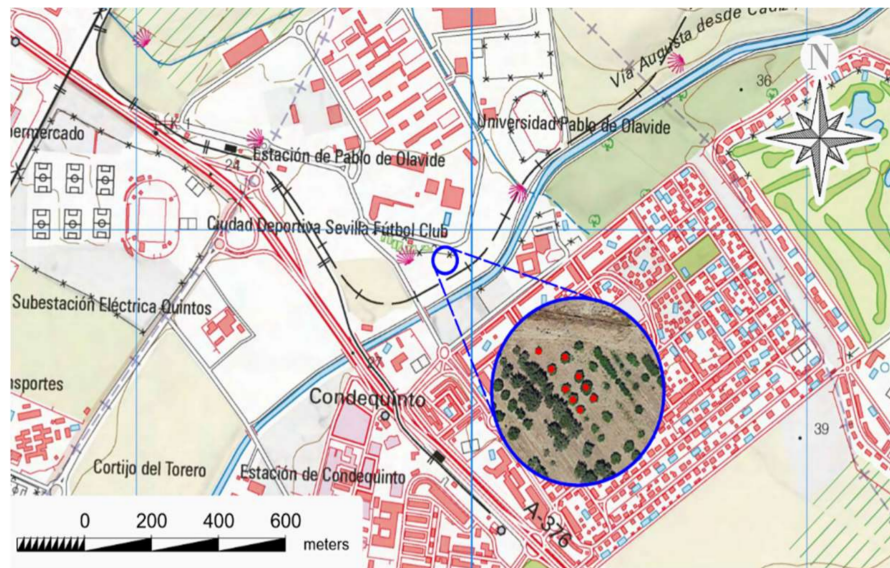


Figure 3. Location of the trials at the University of Sevilla (Spain).

As a control method and to support the different methods used in this study, the coordinates of control points were precisely determined by means of topographic surveying. This was done with the Leica TCR705 (Leica, Wetzlar, Germany) total survey station with an accuracy specified for this surveying equipment of 5" (1.5 mgon) angular and 2 mm + 2 ppm linear. A total of 32 points were determined by positioning on known coordinate points. Of these control points, 9 were of high precision because they were measured on stakes and using a clamp tripod in this way plumbing errors are avoided. After the targets would be placed also on a clamp tripod for data collection with the scanner. Another 14 points were taken on nails that fixed paper targets in A3 format to the ground and that will serve as ground control points (GCP) also called field support points. The control points are reference points that are physically placed in the environment, in our case were photographed from the air with the flight of the UAV, the criterion is that they are visible and easily identifiable in the aerial photos, so targets are placed on the ground for this purpose, its purpose is to generate a correspondence between the ground coordinates of the centre of projection of the photograph, in analytical photogrammetry is known as coplanarity condition equation, and allow the three-dimensional reconstruction of the object. And finally, 9 points taken in the upper part of the treetops that will serve as support points for the images captured from Google Maps (GM).

The reference system used in this work is the official one in Spain, the ETRS89 (European Terrestrial Reference System 1989) which coincides with the WGS84 (World Geodetic System 1984) used by the GPS (Global Positioning System), and the heights are orthometric, i.e., above sea level.

3. Methods

3.1. Traditional Method (TM)

The traditional method is based on assuming that the tree crown is a regular geometric figure like a spheroid [58], in our case we will adopt an ellipsoid that has been used in orange trees [59] and even other kinds of trees like olive trees [13]. Of course, other manual methods are more precise, but also much more laborious, for example, the one proposed by Zaman Salyani [60], which consists of measuring the 6 diameters and 4 heights, but we estimate that it is too complex and not very useful for our study. The intention is to substitute this method if the proposed one turns out to be favorable.

Our study used the ellipsoid which is a closed curved surface whose three main orthogonal sections are ellipses (Figure 4). Once the three semi-axes have been measured, the volume is immediately calculated, although they will also be integrated into drawing programs for comparison purposes. The volume formula used was that of Equation (1). Note that in Figure 3 it seems that the ellipsoid in

some parts the branches and the leaves come off the surface, this is because the ellipsoid obtained by the traditional method has been represented on the model obtained by the HDS method.

$$V_e = \frac{4\pi}{3} a_y b_x c_z \quad (1)$$

being V_e the ellipsoid volume, a_y , b_x , c_z are the semi-axes of the ellipsoid.

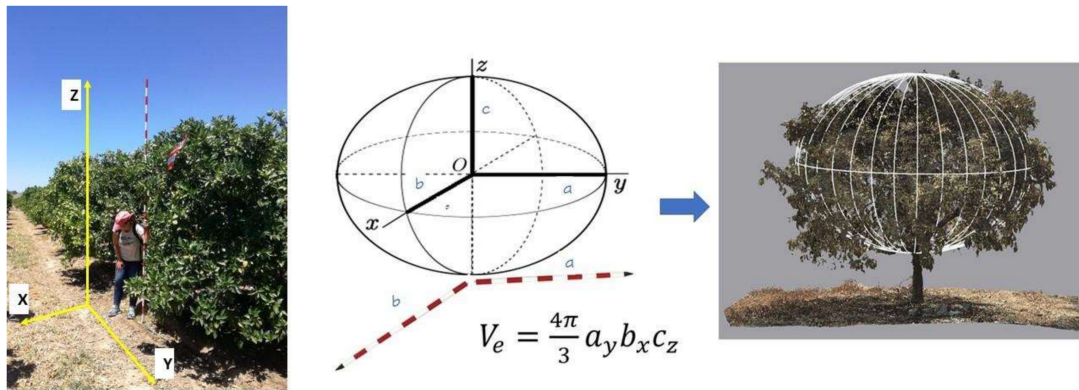


Figure 4. The traditional method for tree crown size assessment. a_y , b_x , c_z are the semi-axes of the ellipsoid, Equation (1).

In the case of the study, the directions of the axes have been defined according to the direction of the crop lines, Figure 4. The Y-axis is the direction of the crop line, the X-axis is the line perpendicular to the crop line (Figure 5), and the Z-axis is the height of the tree. The measurements were made using a tape measure attached to a ranging rod, so that the points to be measured, especially the height, can be easily reached. Figure 4 shows the measurement in the x-direction.



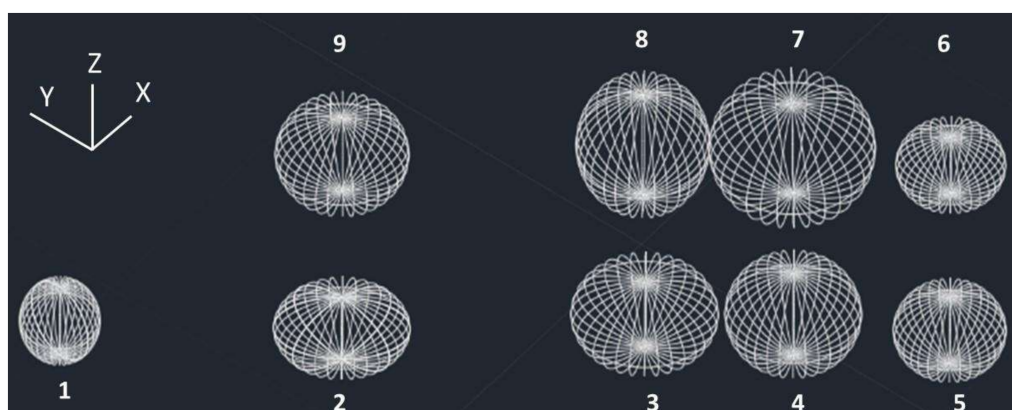
Figure 5. Tree crown size measurement by traditional method. b_x is the semi-axis of the ellipsoid, Equation (1).

The data obtained by the traditional method are shown in Table 1. A total of one hour was used to obtain these measurements in the plot.

Table 1. Traditional method (TM) results. a_y , b_x , c_z are the semi-axes of the ellipsoid, Equation (1).

Tree	b_x	a_y	c_z	Volume (m^3)
1	1.01	1.07	1.13	5.067
2	1.46	1.81	1.02	11.235
3	1.90	1.95	1.05	16.295
4	1.76	1.81	1.35	18.014
5	1.43	1.50	1.09	9.761
6	1.41	1.46	0.93	7.949
7	2.36	2.20	1.48	32.079
8	1.93	1.77	1.64	23.396
9	1.82	1.77	1.20	16.081

To display the volume, the AutoCAD software (Autodesk, Mill Valley, California, USA) was used (Figure 6), where the ellipsoids are displayed in 3D for later comparison with the other methods. The measured semi-axes X and Y of each ellipsoid are incorporated as individual ellipses in each of their corresponding axes. Subsequently, revolutions are made to each ellipsoid, after once the ellipsoid is done, it is scaled with reference to the Z-axis obtained value. Finally, a coordinate change is made for each of the ellipsoids, placing them in their coordinates. The time required in this computer work has been 2 h for the whole process.

**Figure 6.** Results displaying the traditional method (TM). The numbers mean the tree number for Table 1.

3.2. Aerial Photogrammetry (UAV)

In our study, the photogrammetric method was carried out by means of a UAV flight at a determined and constant height. The UAV was equipped with a camera with which sequential photographs are taken respecting a certain overlap between them and following a programmed route. In this case, a “DJI” UAV, model “Mavic Pro” (SZ DJI Technology Co., Ltd., Shenzhen, Guangdong, China) whose camera sensor is 1/2.3” (CMOS), effective pixels: 12.35 M (total pixels: 12.71 M) has been used. PhotoScan software (Agisoft LLC, St. Petersburg in Russia) was used for information processing.

The proposal of more than one flight is conditioned by the distance of the tree plantation frame which forced to fix a higher than usual camera inclination. To ensure that enough information is taken to generate the tree crown models, a multiple flight plan was chosen, since the double grid flights that are usually implemented in flight scheduling applications only allow for one cross grid. A flight plan is made delimiting the zone or work area (Figure 7). Five flight paths were needed to obtain an optimal area, with photographs of all the views of each tree. This is achieved by changing the angle of the camera, and thus the application of the UAV flight calculates the new paths adapted to this new angle.

Figure 7 shows the area under study and the flights made. In this way, path 1, Figure 7A, corresponds to the path taken over the working area. It is not possible to obtain the four sides of the volume with pass 1 alone. It is therefore supplemented by four further paths from outside of the covered area due to the camera inclination as can be shown in Figure 7B, where the green area is the field under study, and white lines the flight trajectory, i.e., the path up, down, left, and right with respect to the working area or zone. Passes 2 to 5 are those corresponding to the four sides of the square (Figure 7B).

The flight plan with the UAV for the vertical photographs, and being able to obtain an accuracy of 0.66 cm/pixel (GSD or Ground Sample Distance) was 20 m height above ground, 80% overlap between photographs and between flight lines, and all with 2 m/s flight speed. The remaining passes were programmed in the same way, except that the angle of the camera was 45° towards our object of study, the orange trees.

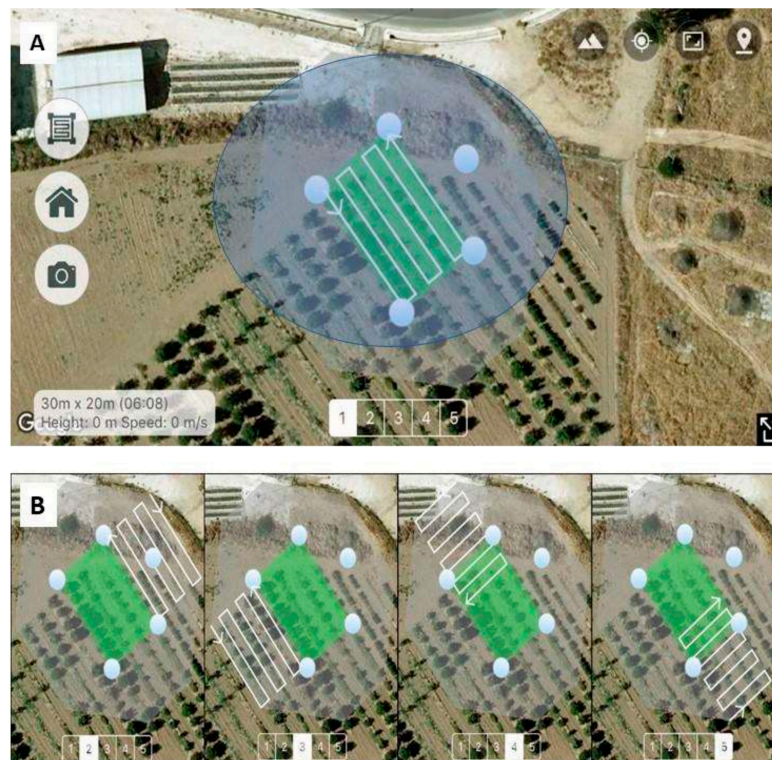


Figure 7. Unmanned aerial vehicle (UAV) paths: (A) Vertical flight; (B) Flights for oblique photographs.

The plot to be flown has an area of 600 m². This was covered with a photographic flight with UAV. For the 5-pass flight, the time needed to perform the flight was 30 min and 40 s. A total of 171 images were obtained. This program uses calculation algorithms based on SfM (Structure from Motion) techniques and performs a range of semi-automatic processes. The process was as follows: a dense point cloud was obtained, formed by a total of 2,691,196 points. With the 14 ground control points (GCP) the model was georeferenced. With these data, the software got an average error of 0.0393 m in coordinates with an accuracy of 0.005 m and with an error of 1.41 pixel. One process to take into account, due to its importance in the final result, is the orientation of the images based on the bundle adjustment, which allows the spatial relocation of both a series of coincident points between images and the positions of the cameras that took those images with respect to the scene.

This process was based on the checkpoints initially measured with the total station, those taken on nails in the targets. Another important part is the creation of the mesh (Figure 8A), in which the calculation algorithm must be chosen, depending on the type of element to be modelled. In our case, the type of surface selected was “arbitrary” because it approximates the result much better to the

reality of the object. Finally, to obtain a higher resolution of the object, giving it a greater impression of realism and detail, the texture is processed (Figure 8B).

Once the whole process is done, all the images of the trees are clipped individually, leaving only the crown or aerial part of the tree. At the end, the images of the treetops are exported as a file with extension .obj to be able to treat it later and calculate its volume. The time needed for information processing was 24 h, with 95% of that time being used for processing.

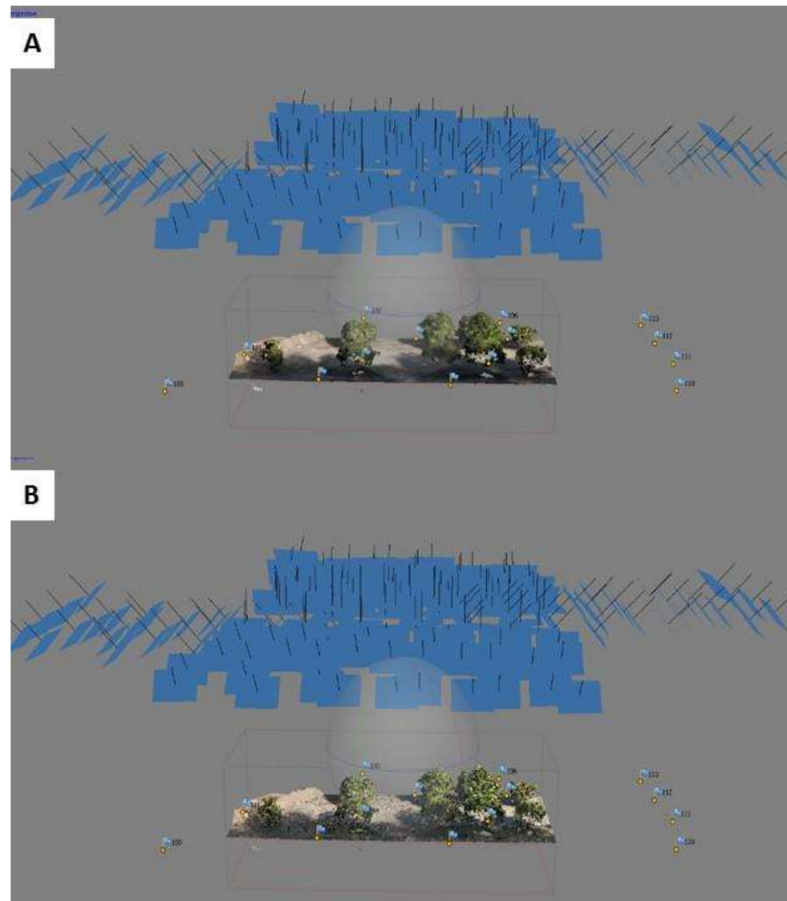


Figure 8. Model from UAV: (A) Mesh; (B) Texture.

3.3. High Definition Survey (HDS)

Since the introduction of Light Detection and Ranging (LiDAR) technology, through HDS (High Definition Survey) there is now a means to quickly digitize the complex structural details of tree crowns [44]. The method with HDS laser scanners is based on the use of a scanner station able to carry out topographic surveys using the “High-Definition Survey” system. The principle of the scanner station is to emit a laser pulse towards an object that bounces back to the station. In this way the station returns a 3-dimensional point cloud of the scanned area. To scan an object with several faces, it is necessary to make several scans from different positions to remove shadows or hidden faces that may arise.

This system allows the reconstruction of complex tree crown geometries thanks to the high density of measured points. These techniques have also been used to measure the crown of orange trees [3]. In this last work, the comparison with traditional or manual methods is outlined. Two types of tree crown volume estimation inspired by manual or traditional methods were tested. The first, named the cube-fit method which is the most common among Brazilian orange growers, consisted of measuring the volume of a cube that contains the whole tree. The second, named cylinder-fit method, consider the volume of the crown as two-thirds of the volume of a cylinder that contains the

tree. The authors themselves state that the dimensions of the cube and the cylinder often produce uncertain measurements due to the difficulty of visually defining the crown borders. In summary, they concluded that LiDAR-based approaches provided a more accurate crown representation than the current manual methods and should be used as a new standard for crown volume calculations.

In our study a Leica brand scanner, model P20, Figure 9A, with linearity error <1 mm and vertical and horizontal angular accuracy $8''/8''$ ($40 \mu\text{rad}/40 \mu\text{rad}$) as accuracy specifications defined by the manufacturer. The targets with their ranging rod and tripods were placed on the stakes visible from the station (Figure 9B). Ten stations with their corresponding scans were made, the total time spent was four hours.

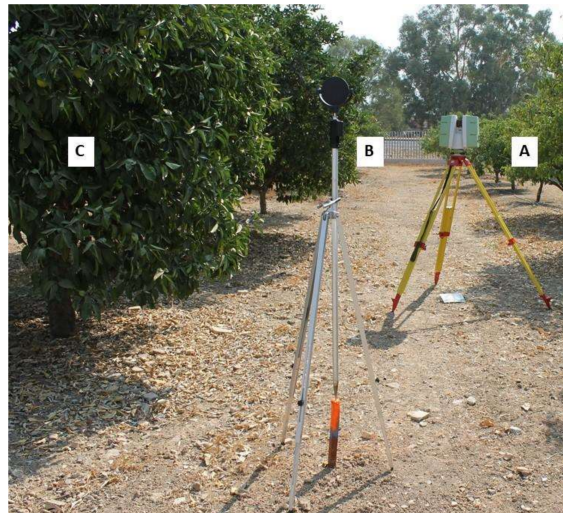


Figure 9. High definition survey (HDS) in the trial. (A) HDS Station. (B) Ranging rod and tripods placed on the stakes. (C) Orange Trees.

Once the data has been collected with HDS, it is processed using Leica's software, "Cyclone" (). Initially, a point cloud is obtained in which the positions of the stations are shown with their reference coordinates and a large point cloud, Figure 10A. Since much more than necessary has been scanned, everything that is not of interest is clipped, resulting in Figure 10B. In Figure 10C, an example of tree number 2 is shown isolated from the rest, and in Figure 10D only the crown of this tree.

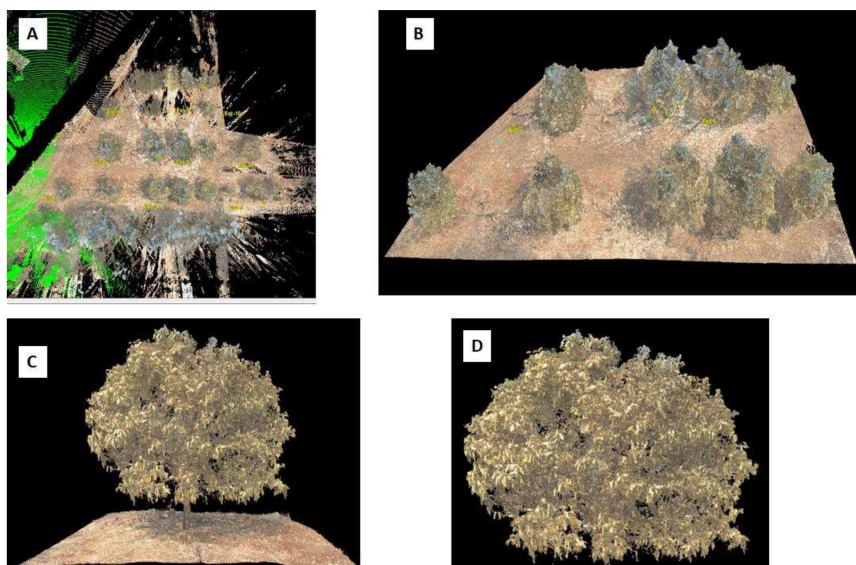


Figure 10. Model from HDS. (A) High-density point cloud. (B) Clipped point cloud. (C) Whole tree 2. (D) Tree crown 2.

Each tree is a cloud of points that are exported as a file (.ptx) so that it can be processed later to calculate its volume. This process took 2 h to perform the entire process including data download, area delimitation and trunk clipping. To calculate the volume of the crown, the “CloudCompare” software (Open Source Project by Daniel Girardeau-Montaut dgirardeau, Grenoble, France) was used. This generates a 3D model with the point cloud of each of the tree crowns obtained. After going through several processes, such as normal curvature estimation, generation of the new model, a model is obtained that is exported to a file (.ply), finally the volume was obtained with the software “3DReshaper” (Leica, Wetzlar, Germany).

3.4. Proposed Method Using Google Maps (GM)

To determine the geometric properties of an object by photogrammetric techniques, such as volume or surface, it is first necessary to obtain the information obtained from several images (usually photographs) from various points of view to reconstruct the geometry. The proposed methodology proposes to replace the aerial photography of UAVs in the field with the use of images extracted from GM. These images are obtained through screenshots of the GM views, as there is no service for downloading views from the GM platform. The concept is to simulate a flight with UAV, so two types of images must be taken (Figure 11), the nadiral image of the zone, and images close to 45 degrees of inclination around the study zone. In this study, 32 images were collected, which were subsequently clipped and saved in an image (.jpg) format file. Figure 12 shows an example of the images acquired at 45° from different points of view. The images obtained from GM had a resolution of 3.96 cm/pixel.

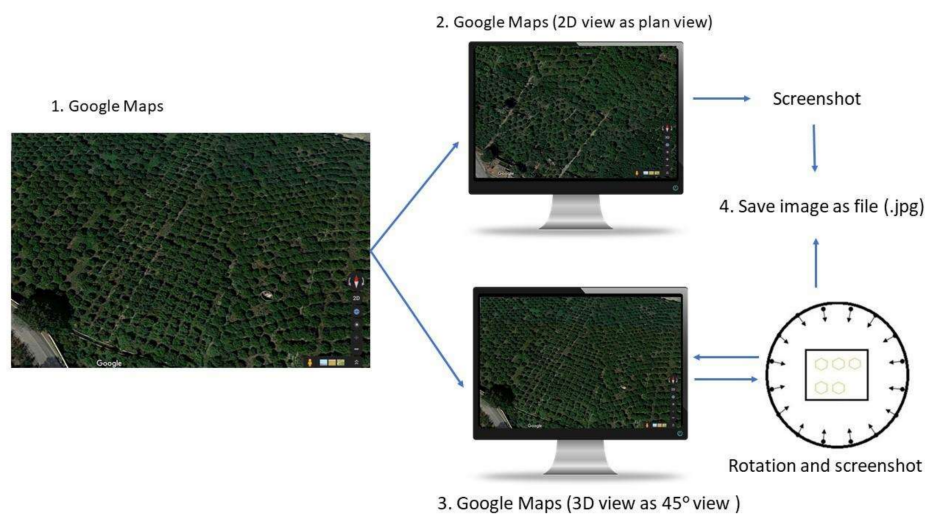


Figure 11. Methodology chart for the proposed method using Google Maps (GM).

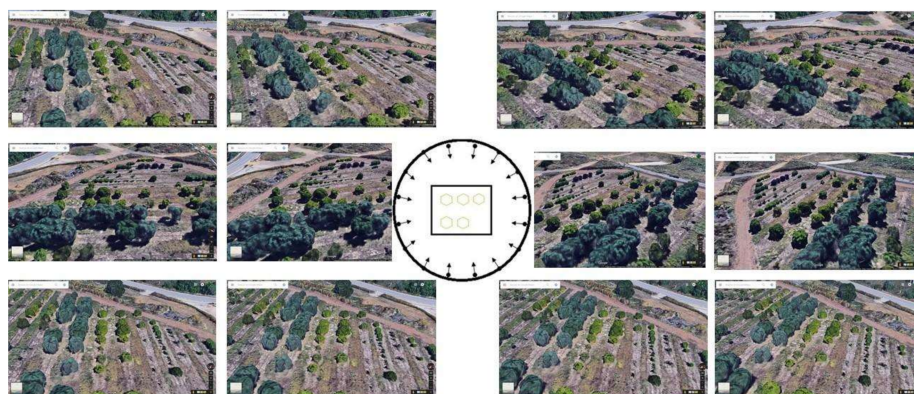


Figure 12. Example of images captured from GM.

The Agisoft Photoscan SW, now called Metashape (Agisoft LLC, St. Petersburg in Russia), was used to process the 32 images. This program uses SfM techniques to obtain 3D modelling of the photographed object or area. To generate precise and well-georeferenced models, once all the images are oriented, the control points taken are placed in the treetops so that with them the final model is optimal in terms of its metrics and positioning in space. In terms of time, no more than 15 min are spent due to the low number of photos and control points. In this process, 619,062 points were obtained once the high-density point cloud was generated. Previously, the control points were located and verified on the crown of the trees, generating an error in coordinates of 0.3716 m and an error of 9.398 pixels.

The results obtained with GM are shown in Figure 13, where for the smallest tree no model has been obtained, tree number 1. On the top of the tree crowns are the location of the checkpoints which have helped to give good accuracy and georeferencing to the final model, Figure 13C. This process is the same as the one performed in the UAV method since the same software is used. The only difference is that for GM, 32 images were obtained, as opposed to the 171 obtained in the UAV method, a significantly lower amount, so the processing time did not exceed 15 min. The result is a textured model, Figure 13C, from which the image of each of the trees, except tree number 1, is extracted, the trunks are clipped and thus we have the area of interest formed by a cloud of points, this cloud is exported with .obj extension to calculate its volume. The software used to generate the 3D mesh from which the volumes are obtained applies a convex envelope algorithm, which removes the inner points of the cloud using only those located on the outer surface.

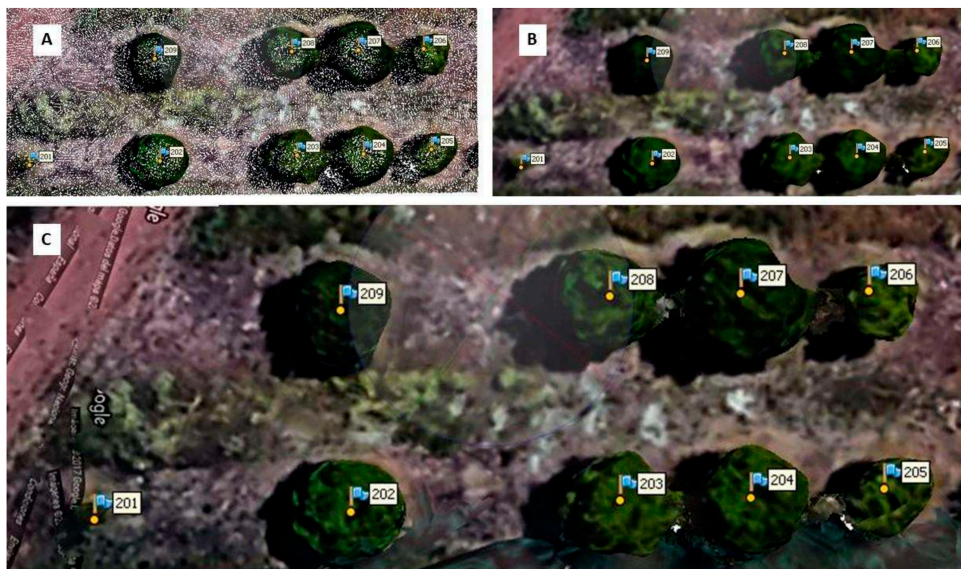


Figure 13. Model from GM. (A) High-density point cloud. (B) Clipped point cloud. (C) Textured model.

3.5. Statistical Analysis

With the results obtained, a statistical analysis will be performed with the XLSTAT 2019 software (Addinsoft, Bordeaux, France). First, the conditions of homoscedasticity and normality will be checked. If it is completed, an ANOVA test will be performed with an interval significance of $p < 0.05$ (5%) and a tolerance of 0.0001. After a Bonferroni test will be performed with $p < 0.05$.

4. Results

To unify all the models obtained with the different methods under study and to be able to analyse the results, the “3DReshaper” software was used. This software is capable of processing point clouds and 3D models and calculating the volume of each one. The sensitivity of the volume calculation is not specified by the 3DReshaper manufacturer. As it is a mathematical calculation, the accuracy depends on the number of points that define the outer surface, as it is an irregular surface, the greater

the density of points, the better defined the irregular surface of the tree crown will be. The models of the trees obtained by the four methods used were introduced. As the results of the GM method show, it was not possible to detect the small tree. Therefore, a total of 32 models are available for comparative analysis. Figure 14 shows an overlap of these models. A detail of these can be seen in Figure 15 for tree number 7. In Figure 15, the ellipsoid obtained with the traditional method has been maintained in each of the models to make a visual reference.

Table 2 summarizes all the volumes obtained with the “3DReshaper”, where the trees have been sorted by crown size for further error analysis according to tree size. Firstly, it has been observed that the GM method has not been able to detect the smallest tree, so it is not advisable for tree crowns below 5 m³.

Secondly, the traditional method offers the highest results, whatever the tree observed compared to the other methods. Note that volumes of treetops have been found to be higher depending on the method. This is attributed to the geometry of the tree, which may favour one or the other method. In general, the resulting values could be ordered roughly as follows according to the volumes obtained: TM >> GM > UAV > HDS. This suggests that the more accurate the method is, the smaller the volume achieved for the crown of the tree, probably because methods that involve fewer data are more roughly.

The crown of a real tree is an imperfect three-dimensional representation with depressions and projections. On the other hand, the mathematical representation used is that of a perfect ellipsoid, defined by its three semi-axes measured in the field. In Figure 15, by the TM it can be seen how the ellipsoid encompasses the top of the tree, but nevertheless, some branches extend from it, due to the nature of the tree itself. This geometrical figure has proven to be better than the models used by Brazilian orange producers. In this figure, it can be appreciated how there are gaps between the real contour of the tree and the ellipsoid. The problem that arises is that the ellipsoid itself uses these cavities for the calculation of the tree’s crown instead of deleting them (Figure 16). In this way, whether the volume of the ellipsoid is greater or lesser, it will always calculate the volume by excess or by default and that is why it will not faithfully represent what is real. To illustrate the issue of excess volume of the TM, the cross-sections have been marked in red in Figure 16, for a front (Figure 16A) and side (Figure 16B) views. Figure 16C shows a top view with the leaves and the TM and Figure 15D show only the contours, which will be used later in the sections of Figure 17. In Figure 17 some of these cross-sections of tree 7 have been represented, where they are compared with the contour of the leaves, determined by the HDS method. Note that the sections are listed with the height above sea level and that the lowest point in the crown of this tree is 22.1 m above sea level. To illustrate a final example of the large approximation involved in the TM, a variation of 10 cm in one of the measurements of the tree 7, e.g., the measurement of the tree height, results in a variation of 10% i.e., 3 m³. Figure 18 illustrates the results obtained in Table 3 as a function of the absolute volume of the tree. Figure 18 also shows the trend lines of the methods.

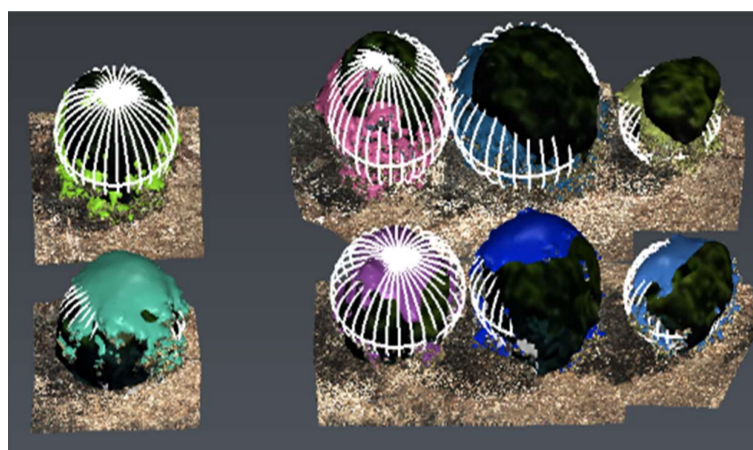


Figure 14. Overlapping of models created with 3DReshaper.

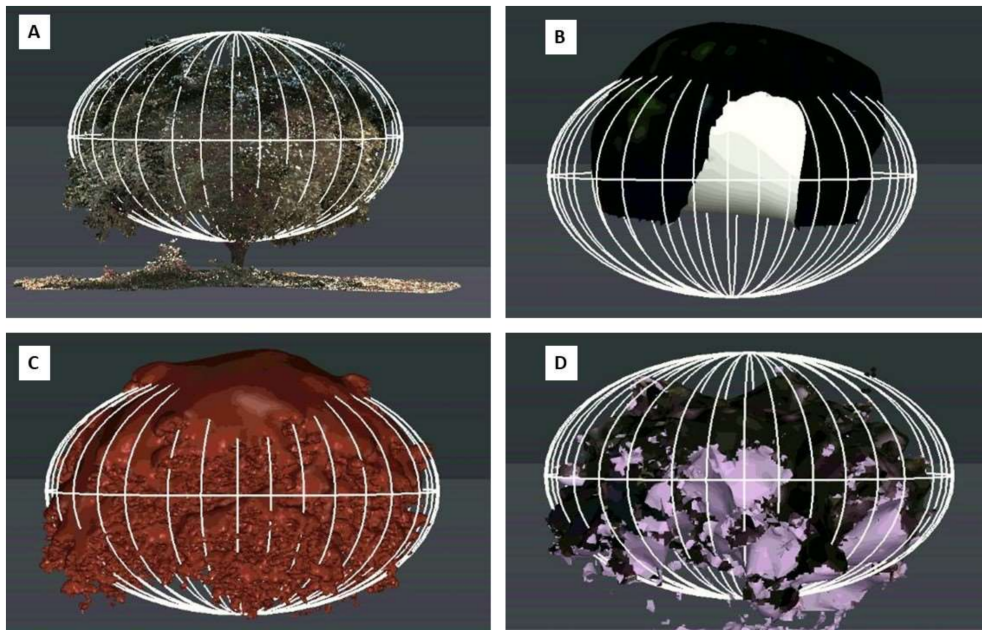


Figure 15. Visual assessment of the different methods for tree 7. (A) TM vs. tree. (B) UAV vs. TM. (C) HDS vs. TM. (D) GM vs. TM.

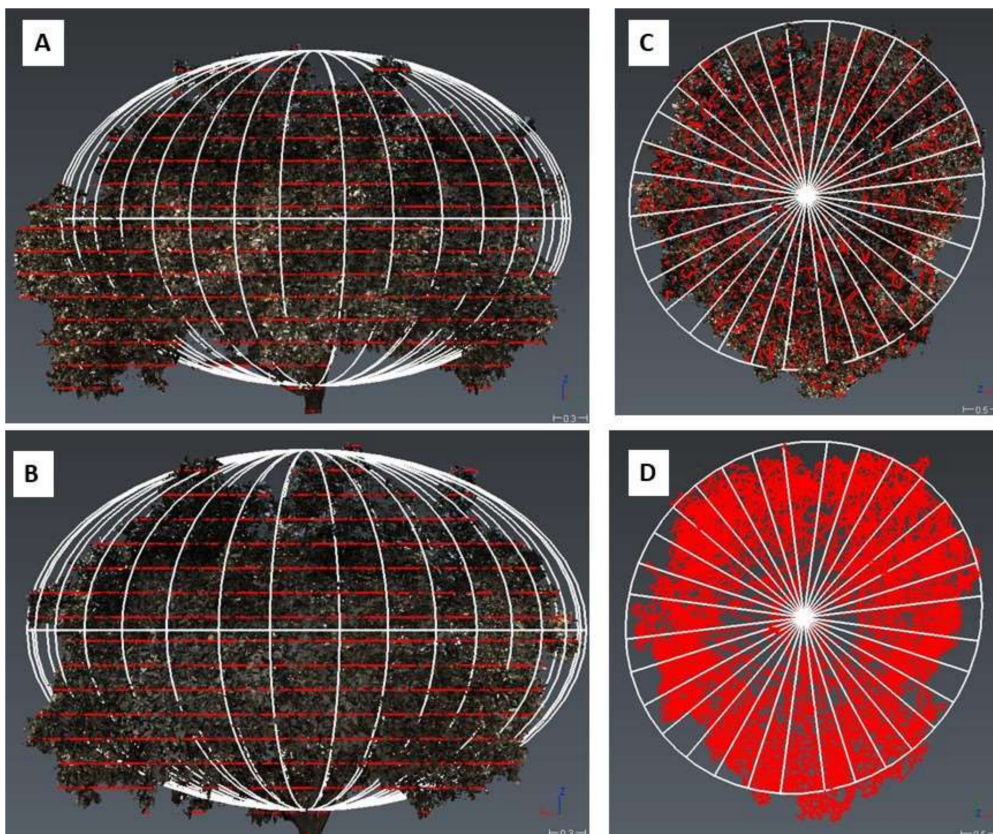


Figure 16. The visual composition of the TM (ellipsoid) and the HDS for tree 7, the red lines mark the cross-sections. (A) Frontal view. (B) Side view (left-right). (C) Top view (with leaves). (D) Top view (contour).

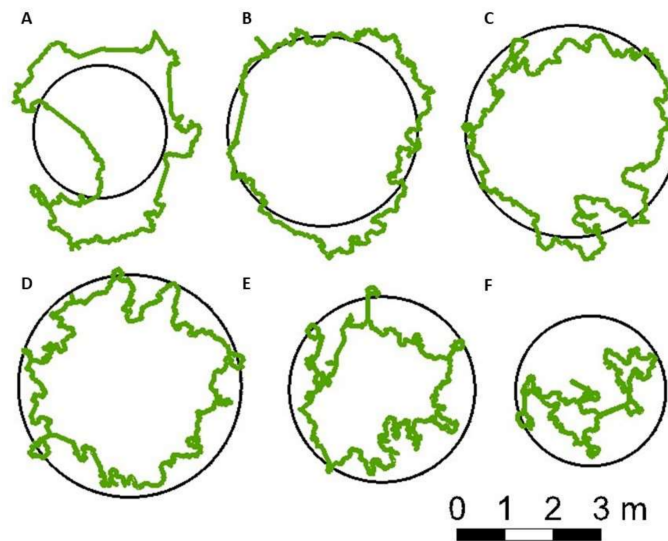


Figure 17. Cross-sections at different heights (above sea level) of tree 7 for TM and HDS (contour). (A) Cross-section at 22.4 m. (B) Cross-section at 23 m. (C) Cross section at 23.4 m. (D) Cross-section at 24 m. (E) Cross-section at 24.5 m. (F) Cross-section at 24.7 m.

Table 2. Results of the crown volumes (m³) of the orange trees with each of the methods studied.

Tree	TM	GM	UAV	HDS
1	5.067	N/A	2.866	3.172
6	7.949	5.005	3.591	3.797
5	9.76	5.741	3.378	5.378
2	11.235	12.343	8.712	6.854
9	16.081	10.092	11.991	7.737
3	16.295	10.466	5.237	6.814
4	18.014	16.18	9.53	9.676
8	23.4	16.655	14.329	9.926
7	32.079	18.844	17.151	13.952

TM (Traditional Method); GM (Google Maps); UAV (Unmanned Aerial Vehicle); HDS (High Definition Survey).

Table 3. Volume error with respect to the reference method (HDS).

Tree	TM		GM		UAV	
	Error (m ³)	%	Error (m ³)	%	Error (m ³)	%
6	4.152	109.3	−0.206	−5.4	1.208	31.8
5	4.382	81.5	−2	−37.2	0.363	6.7
3	9.481	139.1	−1.577	−23.1	3.652	53.6
2	4.381	63.9	1.858	27.1	5.489	80.1
4	8.338	86.2	−0.146	−1.5	6.504	67.2
9	8.344	107.8	4.254	55.0	2.355	30.4
8	13.474	135.7	4.403	44.4	6.729	67.8
7	18.127	129.9	3.199	22.9	4.892	35.1
Average		106.7		10.3		46.6
SD		27.6		32.4		24.6

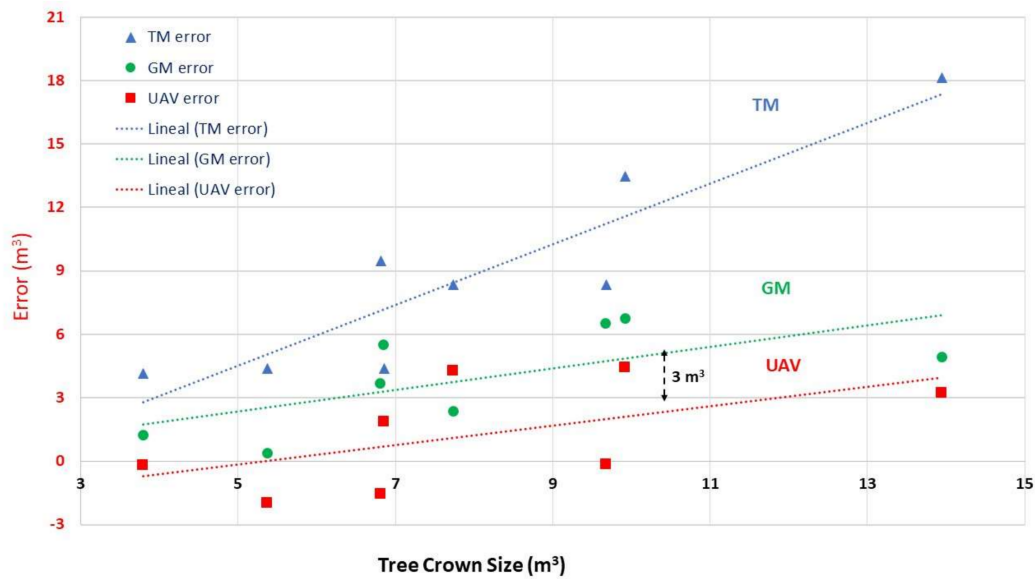


Figure 18. Volume error (m³) related to absolute tree crown size.

Once the conditions of normality and homoscedasticity were checked, the ANOVA test was performed. The results of the Bonferroni test are shown in Table 4.

Table 4. Statistical analysis of the 4 methods.

Method	Least Squares Means (Volume)
HDS	7.478 a
UAV	8.532 ab
GM	11.916 ab
TM	15.513 b

Numbers with different letters in the column are different ($p < 0.05$; Bonferroni test).

5. Discussion

Figure 19 shows the progress of the research on the estimation of tree crown volume. It can be appreciated that the first techniques were based on aerial photography as the used in fifth inventory of the U.S. Forest Service [61]. Photogrammetric modelling of a tree from terrestrial stereo-photography was used from a long time ago [62]. Further, it has been done using aerial photogrammetry. There are numerous studies in the literature showing the benefits of the latter method. The first research was based on classical aerial photogrammetry, for example, on apple trees with Panchromatic images and 1:4000 scale, to obtain a DEM (Digital Elevation Model) of the crop [9]. And more recently, low-cost systems such as UAVs have been used for these purposes [63,64]. LiDAR canopy characterization was also used early in forests highlighting that most crowns were asymmetrical for Queensland maple [65].

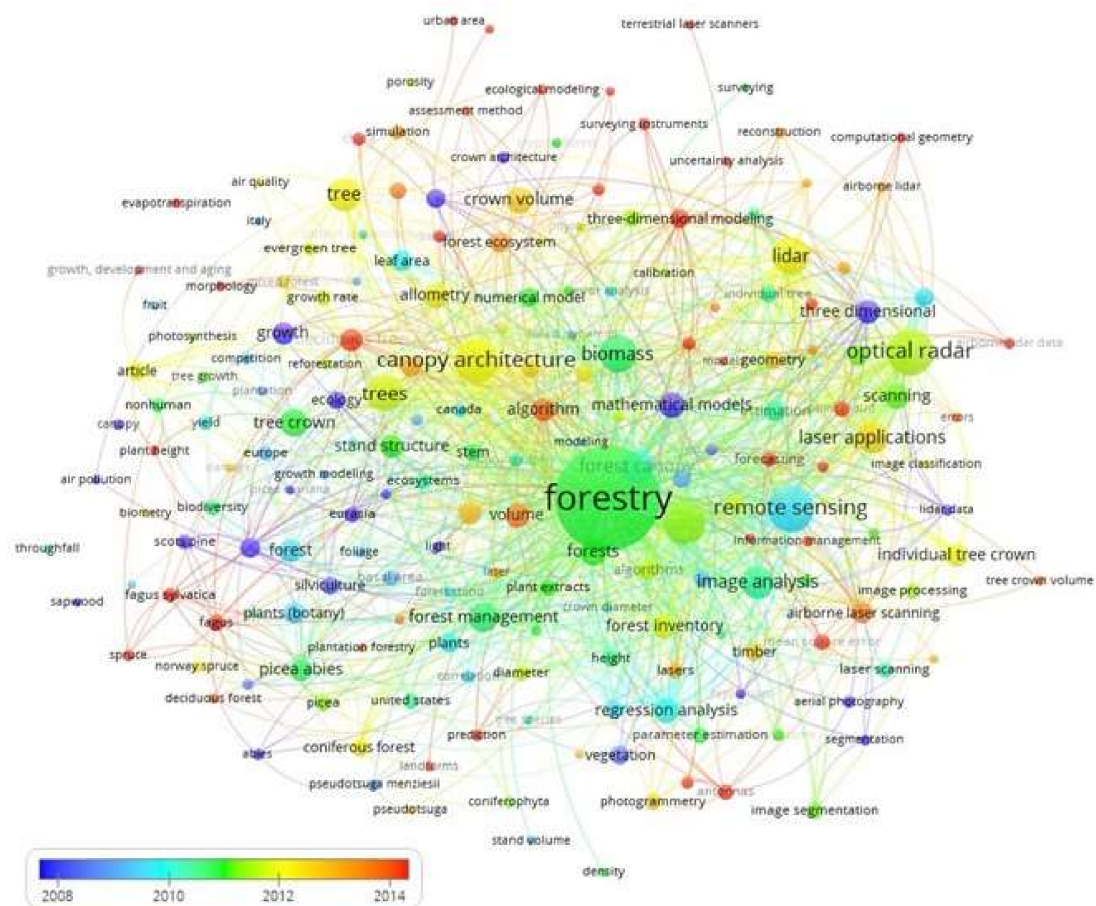


Figure 19. Research trend evolution to tree crown volume estimation.

According to the literature reviewed, the most accurate method of all is the one that uses the HDS [13] and therefore is the one used as a reference for the calculation of the relative error, obtaining Table 3. Here the deviations are obtained in % of the volume of the tree itself, taking as a reference volume that of the HDS. It can be seen that, on average, the TM has a 100% error, although the result may seem excessive, this is no surprise, since it is still lower than what other similar studies obtain, as the one carried out in Brazil also for orange trees obtaining approximately 150% larger than the volume from the LiDAR techniques [66,67], of course in this work the traditional methods of approximation are unrealistic (cube fit or cylinder-fit), but they are the ones used by the growers.

The UAV method has the lowest error as expected, on average 10%. So, also considering cost, it is clear that it is a very good method. The proposed GM method has proved to have an average error of less than 50%. It is therefore an alternative method to traditional methods, with the added advantages that the images are free. In addition, due to civil aviation rules, for example in Spain, there are many restricted areas for the flight of UAVs.

Figure 20 summarizes the results obtained using the Bonferroni test (Table 4). As can be inferred from the statistical analysis, photogrammetric methods, i.e., UAV or GM, do not differ significantly from either TM or HDS. But the latter two, TM and HDS are significantly different from each other. If the LS means are observed, it can be seen, as was previously deduced qualitatively, which method is more precise: HDS, followed by UAV, GM and finally TM.

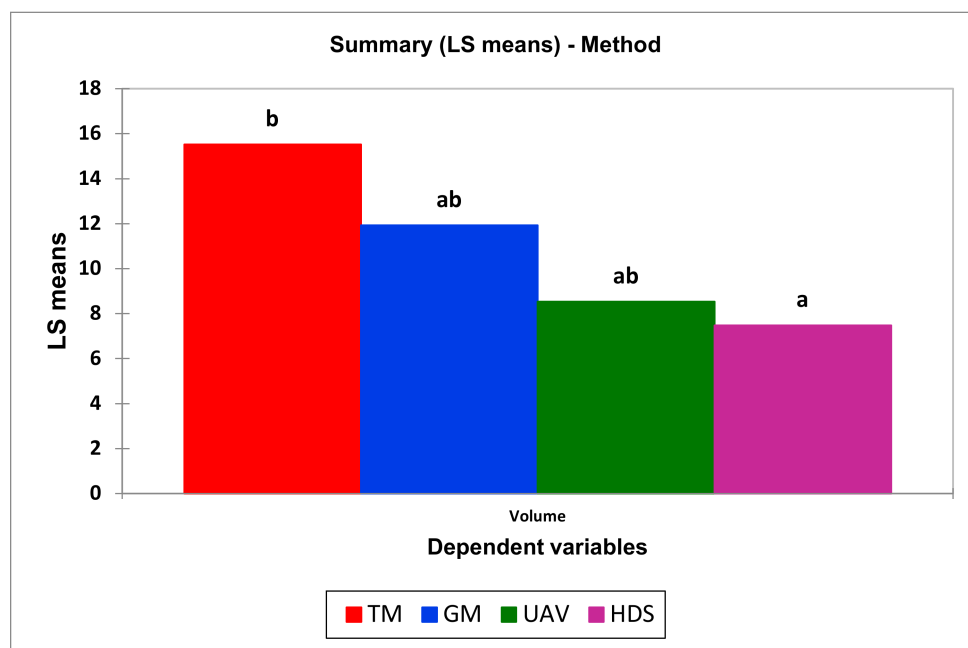


Figure 20. Statistical analysis of the methods used (Bonferroni test). TM (Traditional Method); GM (Google Maps); UAV (Unmanned Aerial Vehicle); HDS (High Definition Survey).

6. Conclusions

The estimation of the volume of the treetops in general and of the orange trees, in particular, is an important subject of study for agriculture for the dosage of treatments, for the calculation of the biomass, or the calculation of the irrigation rates. The traditional methods have been replaced by more accurate methods, at first terrestrial photogrammetry, then aerial photogrammetry, and lately the HDS or TLS have appeared, and with the decrease in the price of UAVs, aerial photogrammetry has re-emerged but now at a low cost. Unfortunately, it is not always possible to carry out UAV flights throughout the territory, such as areas near airports, urban areas, or restricted areas in general.

In this research, the option of using GM images as a photogrammetric flight has been assessed, for situations in which it is not possible to fly with UAVs. After a statistical analysis of the results, it has been observed that the HDS method is the most accurate, followed by the UAV flight, then the proposed method using images from Google Maps (GM) and finally the traditional method measuring tree crown parameters in the field and approximating geometric figures. The two photogrammetric methods, with UAV and with GM, present significant differences between them, neither with the traditional methods nor with the HDS, then they can be used to compare them. However, there are significant differences between the traditional method and the HDS.

Finally, it is necessary to be aware of the limitations found in this study, firstly that the updating of GM is not carried out periodically, and secondly the restriction for trees smaller than 5 m³ in volume. This work opens new opportunities to explore images from massive mapping platforms such as Google Maps for the assessment of tree crown volumes.

Author Contributions: Conceptualization, C.M.-B. and A.P.-R.; methodology, C.M.-B., A.P.-R., and F.M.-A.; resources: C.M.-B., F.T.-Á., and A.P.-R.; data collection, C.M.-B., F.T.-Á., and A.P.-R.; formal analysis: C.M.-B., F.T.-Á., and A.P.-R.; writing—original draft, C.M.-B., A.P.-R., and F.M.-A.; supervision, F.M.-A.; writing—review and editing, C.M.-B., A.P.-R., F.T.-Á., and F.M.-A. All authors have read and agreed to the published version of the manuscript.

Funding: This work has been partially supported by the Spanish Ministry of Economy and Competitiveness under the research projects HAR2014-53350-P and HAR2017-86334-R.

Acknowledgments: The authors would like to thank the University of Seville for allowing trials on its plots.

Conflicts of Interest: The authors declare no conflict of interest. Mention of trade names or commercial products in this publication is solely to provide specific information and does not imply recommendation or endorsement by the authors of this article.

References

1. Torres, J.; Valera, D.L.; Belmonte, L.J.; Herrero-Sánchez, C. Economic and Social Sustainability through Organic Agriculture: Study of the Restructuring of the Citrus Sector in the “Bajo Andarax” District (Spain). *Sustainability* **2016**, *8*, 918. [[CrossRef](#)]
2. Zapata-Sierra, A.J.; Manzano-Agugliaro, F. Controlled deficit irrigation for orange trees in Mediterranean countries. *J. Clean. Prod.* **2017**, *162*, 130–140. [[CrossRef](#)]
3. Gimenez, E.; Salinas, M.; Manzano-Agugliaro, F. Worldwide research on plant defense against biotic stresses as improvement for sustainable agriculture. *Sustainability* **2018**, *10*, 391. [[CrossRef](#)]
4. Khelifi, H.; Selmane, R.; Ben Mimoun, M.; Tadeo, F.; Morillon, R.; Luro, F. Abscission of Orange Fruit (*Citrus sinensis* (L.) Osb.) in the Mediterranean Basin Depends More on Environmental Conditions Than on Fruit Ripeness. *Agronomy* **2020**, *10*, 591. [[CrossRef](#)]
5. Whitney, J.D.; Tumbo, S.D.; Miller, W.M.; Wheaton, T.A. *Comparison between Ultrasonic and Manual Measurements of Citrus Tree Canopies*; Paper No. 021052; ASAE (American Society of Agricultural Engineers): St. Joseph, MI, USA, 2002.
6. Doorenbos, J.; Pruitt, W.O. *Guidelines for Predicting Crop Water Requirements*; FAO 24; Food and Agriculture Organization: Rome, Italy, 1977; pp. 1–60.
7. Smith, M.; Monteith, J.L.; Allen, R.G.; Perrier, A.; Perreira, L.S.; Segeren, A. *Expert Consultation on Revision of FAO Methodologies for Crop Water Requirements*; Land and Water Development Division, FAO: Rome, Italy, 1998.
8. Hupert, H.; Gal, Y.; Peres, M. *Irrigation Coefficients and Water Amounts for Deciduous Orchards*; Soil and Irrigation Extension Service, Ministry of Agriculture: Kiriat Shmona, Israel, 1997.
9. Meron, M.; Cohen, S.; Melman, G. Tree shape and volume measurement by light interception and aerial photogrammetry. *Trans. ASAE* **2000**, *43*, 475–481. [[CrossRef](#)]
10. Márquez, A.L.; Baños, R.; Gil, C.; Montoya, M.G.; Manzano-Agugliaro, F.; Montoya, F.G. Multi-objective crop planning using pareto-based evolutionary algorithms. *Agric. Econ.* **2011**, *42*, 649–656. [[CrossRef](#)]
11. Fuchs, M.; Cohen, Y.; Moreshet, S. Determining transpiration from meteorological data and crop characteristics for irrigation management. *Irrig. Sci.* **1987**, *8*, 91–99. [[CrossRef](#)]
12. Padilla, F.M.; Gallardo, M.; Manzano-Agugliaro, F. Global trends in nitrate leaching research in the 1960–2017 period. *Sci. Total Environ.* **2018**, *643*, 400–413. [[CrossRef](#)]
13. Miranda-Fuentes, A.; Llorens, J.; Gamarra-Diezma, J.L.; Gil-Ribes, J.A.; Gil, E. Towards an optimized method of olive tree crown volume measurement. *Sensors* **2015**, *15*, 3671–3687. [[CrossRef](#)]
14. Walklate, P.J.; Cross, J.V.; Richardson, G.M.; Murray, R.A.; Baker, D.E. It–Information technology and the human interface: Comparison of different spray volume deposition models using lidar measurements of apple orchards. *Biosyst. Eng.* **2002**, *82*, 253–267. [[CrossRef](#)]
15. Siegfried, W.; Viret, O.; Huber, B.; Wohlhauser, R. Dosage of plant protection products adapted to leaf area index in viticulture. *Crop. Prot.* **2007**, *26*, 73–82. [[CrossRef](#)]
16. Fernández-Sarría, A.; Martínez, L.; Velázquez-Martí, B.; Sajdak, M.; Estornell, J.; Recio, J.A. Different methodologies for calculating crown volumes of *Platanus hispanica* trees using terrestrial laser scanner and a comparison with classical dendrometric measurements. *Comput. Electron. Agric.* **2013**, *90*, 176–185.
17. Dalponte, M.; Bruzzone, L.; Gianelle, D. A system for the estimation of single-tree stem diameter and volume using multireturn LiDAR data. *IEEE Trans. Geosci. Remote Sens.* **2011**, *49*, 2479–2490. [[CrossRef](#)]
18. Janott, M.; Gayler, S.; Gessler, A.; Javaux, M.; Klier, C.; Priesack, E. A one-dimensional model of water flow in soil-plant systems based on plant architecture. *Plant Soil* **2011**, *341*, 233–256. [[CrossRef](#)]
19. Van Pelt, R.; North, M.P. Analyzing canopy structure in Pacific Northwest old-growth forests with a stand-scale crown model. *Northwest Sci.* **1996**, *70*, 15–30.
20. Yu, X.; Hyypä, J.; Kukko, A.; Maltamo, M.; Kaartinen, H. Change detection techniques for canopy height growth measurements using airborne laser scanner data. *Photogramm. Eng. Remote Sens.* **2006**, *72*, 1339–1348. [[CrossRef](#)]

21. Rautiainen, M.; Möttöus, M.; Stenberg, P.; Ervasti, S. Crown envelope shape measurements and models. *Silva Fenn.* **2008**, *42*, 19. [[CrossRef](#)]
22. Lindberg, E.; Olofsson, K.; Holmgren, J.; Olsson, H. Estimation of 3D vegetation structure from waveform and discrete return airborne laser scanning data. *Remote Sens. Environ.* **2012**, *118*, 151–161. [[CrossRef](#)]
23. Sharma, R.P.; Vacek, Z.; Vacek, S. Individual tree crown width models for Norway spruce and European beech in Czech Republic. *For. Ecol. Manag.* **2016**, *366*, 208–220. [[CrossRef](#)]
24. Krucek, M.; Trochta, J.; Cibulka, M.; Král, K. Beyond the cones: How crown shape plasticity alters aboveground competition for space and light—Evidence from terrestrial laser scanning. *Agric. For. Meteorol.* **2019**, *264*, 188–199. [[CrossRef](#)]
25. Alonzo, M.; McFadden, J.P.; Nowak, D.J.; Roberts, D.A. Mapping urban forest structure and function using hyperspectral imagery and lidar data. *Urban For. Urban Green.* **2016**, *17*, 135–147. [[CrossRef](#)]
26. Kazmierczak, K.; Zawieja, B. Tree crown size as a measure of tree biosocial position in 135-year-old oak (*Quercus L.*) stand. *Folia For. Pol.* **2016**, *58*, 31–42. [[CrossRef](#)]
27. Díaz-Varela, R.A.; De la Rosa, R.; León, L.; Zarco-Tejada, P.J. High-resolution airborne UAV imagery to assess olive tree crown parameters using 3D photo reconstruction: Application in breeding trials. *Remote Sens.* **2015**, *7*, 4213–4232. [[CrossRef](#)]
28. Song, C.; Dickinson, M.B.; Su, L.; Zhang, S.; Yaussey, D. Estimating average tree crown size using spatial information from Ikonos and QuickBird images: Across-sensor and across-site comparisons. *Remote Sens. Environ.* **2010**, *114*, 1099–1107. [[CrossRef](#)]
29. Falkowski, M.J.; Smith, A.M.; Hudak, A.T.; Gessler, P.E.; Vierling, L.A.; Crookston, N.L. Automated estimation of individual conifer tree height and crown diameter via two-dimensional spatial wavelet analysis of lidar data. *Can. J. Remote Sens.* **2006**, *32*, 153–161. [[CrossRef](#)]
30. Gill, S.J.; Biging, G.S.; Murphy, E.C. Modeling conifer tree crown radius and estimating canopy cover. *For. Ecol. Manag.* **2000**, *126*, 405–416. [[CrossRef](#)]
31. Purves, D.W.; Lichstein, J.W.; Pacala, S.W. Crown plasticity and competition for canopy space: A new spatially implicit model parameterized for 250 North American tree species. *PLoS ONE* **2007**, *2*, e870. [[CrossRef](#)]
32. Goodwin, N.R.; Coops, N.C.; Culvenor, D.S. Assessment of forest structure with airborne LiDAR and the effects of platform altitude. *Remote Sens. Environ.* **2006**, *103*, 140–152. [[CrossRef](#)]
33. Leckie, D.G.; Gougeon, F.A.; Walsworth, N.; Paradine, D. Stand delineation and composition estimation using semi-automated individual tree crown analysis. *Remote Sens. Environ.* **2003**, *85*, 355–369. [[CrossRef](#)]
34. Pretzsch, H.; Dieler, J. Evidence of variant intra- and interspecific scaling of tree crown structure and relevance for allometric theory. *Oecologia* **2012**, *169*, 637–649. [[CrossRef](#)]
35. Popescu, S.C.; Wynne, R.H.; Nelson, R.F. Measuring individual tree crown diameter with lidar and assessing its influence on estimating forest volume and biomass. *Can. J. Remote Sens.* **2003**, *29*, 564–577. [[CrossRef](#)]
36. Breidenbach, J.; Næsset, E.; Lien, V.; Gobakken, T.; Solberg, S. Prediction of species specific forest inventory attributes using a nonparametric semi-individual tree crown approach based on fused airborne laser scanning and multispectral data. *Remote Sens. Environ.* **2010**, *114*, 911–924. [[CrossRef](#)]
37. Albrigo, L.G.; Anderson CA; Edwards, G.J. Yield estimation of ‘Valencia’ orange research plots and groves. *Proc. Fla. State Hortic. Soc.* **1975**, *88*, 44–49.
38. Wheaton, T.A.; Whitney, J.D.; Castle, W.S.; Muraro, R.P.; Browning, H.W.; Tucker, D.P.H. Citrus Scion and rootstock, topping height, and tree spacing affect tree size, yield, fruit quality, and economic return. *J. Am. Soc. Hortic. Sci.* **1995**, *120*, 861–870. [[CrossRef](#)]
39. Tumbo, S.D.; Salyani, M.; Whitney, J.D.; Wheaton, T.A.; Miller, W.M. Investigation of laser and ultrasonic ranging sensors for measurements of citrus canopy volume. *Appl. Eng. Agric.* **2002**, *18*, 367–372. [[CrossRef](#)]
40. Stajniko, D.; Berk, P.; Lešnik, M.; Ježič, V.; Lakota, M.; Strancar, A.; Hočevar, M.; Rakun, J. Programmable ultrasonic sensing system for targeted spraying in orchards. *Sensors* **2012**, *12*, 15500–15519. [[CrossRef](#)] [[PubMed](#)]
41. Rosell, J.R.; Sanz, R. A review of methods and applications of the geometric characterization of tree crops in agricultural activities. *Comput. Electron. Agric.* **2012**, *81*, 124–141. [[CrossRef](#)]
42. Gil, E.; Escolà, A.; Rosell, J.R.; Planas, S.; Val, L. Variable rate application of plant protection products in vineyard using ultrasonic sensors. *Crop. Prot.* **2007**, *26*, 1287–1297. [[CrossRef](#)]
43. Llorens, J.; Gil, E.; Llop, J. Ultrasonic and LIDAR sensors for electronic canopy characterization in vineyards: Advances to improve pesticide application methods. *Sensors* **2011**, *11*, 2177–2194. [[CrossRef](#)]

44. Escolá, A.; Planas, S.; Rosell, J.; Pomar, J.; Camp, F.; Gracia, F.; Llorens, J.; Gil, E. Performance of an Ultrasonic Ranging Sensor in Apple Tree Canopies. *Sensors* **2011**, *11*, 2459–2477. [[CrossRef](#)]
45. Méndez, V.; Pérez-Romero, A.; Sola-Guirado, R.; Miranda-Fuentes, A.; Manzano-Agugliaro, F.; Zapata-Sierra, A.; Rodríguez-Lizana, A. In-Field Estimation of Orange Number and Size by 3D Laser Scanning. *Agronomy* **2019**, *9*, 885. [[CrossRef](#)]
46. Perea-Moreno, A.J.; Aguilera-Ureña, M.J.; Larriva, M.D.; Manzano-Agugliaro, F. Assessment of the potential of UAV video image analysis for planning irrigation needs of golf courses. *Water* **2016**, *8*, 584. [[CrossRef](#)]
47. Fernández-Hernandez, J.; González-Aguilera, D.; Rodríguez-Gonzálvez, P.; Mancera-Taboada, J. Image-based modelling from unmanned aerial vehicle (UAV) photogrammetry: An effective, low-cost tool for archaeological applications. *Archaeometry* **2015**, *57*, 128–145. [[CrossRef](#)]
48. Grenzdörffer, G.J.; Engel, A.; Teichert, B. The photogrammetric potential of low-cost UAVs in forestry and agriculture. *Int. Arch. Photogramm. Remote Sens. Spat. Inf. Sci.* **2008**, *31*, 1207–1214.
49. Inzerillo, L.; Leto Barone, F.; Roberts, R. 3D modeling of a complex building: From multi-view image fusion to google earth publication. *Int. Arch. Photogramm. Remote Sens. Spat. Inf. Sci.* **2019**, 577–584. [[CrossRef](#)]
50. Hu, F.; Ge, J.; Lu, C.; Li, Q.; Lv, S.; Li, Y.; Liu, Y. Obtaining elevation of Oncomelania Hupensis habitat based on Google Earth and it's accuracy evaluation: An example from the Poyang lake region, China. *Sci. Rep.* **2020**, *10*, 515. [[CrossRef](#)]
51. González-Delgado, J.Á.; Martínez-Graña, A.; Holgado, M.; Gonzalo, J.C.; Legoinha, P. Augmented Reality as a Tool for Promoting the Tourist Value of the Geological Heritage Around Natural Filming Locations: A Case Study in “Sad Hill” (The Good, the Bad and the Ugly Movie, Burgos, Spain). *Geoheritage* **2020**, *12*, 1–11. [[CrossRef](#)]
52. Wernecke, J. *The KML Handbook: Geographic Visualization for the Web*; Pearson Education: London, UK, 2008.
53. Crampton, J.W. Keyhole, Google Earth, and 3D Worlds: An Interview with Avi Bar-Zeev. *Cartogr. Int. J. Geogr. Inf. Geovis.* **2008**, *43*, 85–93. [[CrossRef](#)]
54. Tsai, V.J.; Chen, J.H.; Huang, H.S. Traffic Sign Inventory from Google Street View Images. *Int. Arch. Photogramm. Remote Sens. Spat. Inf. Sci.* **2016**, *41*, 243–246. [[CrossRef](#)]
55. García-Albertos, P.; Picornell, M.; Salas-Olmedo, M.H.; Gutiérrez, J. Exploring the potential of mobile phone records and online route planners for dynamic accessibility analysis. *Transp. Res. Part A Policy Pract.* **2019**, *125*, 294–307. [[CrossRef](#)]
56. De Vries, S.; Buijs, A.E.; Langers, F.; Farjon, H.; van Hinsberg, A.; Sijtsma, F.J. Measuring the attractiveness of Dutch landscapes: Identifying national hotspots of highly valued places using Google Maps. *Appl. Geogr.* **2013**, *45*, 220–229. [[CrossRef](#)]
57. Hu, S. Online Map Service Using Google Maps API and Other JavaScript Libraries: An Open Source Method. In *Online Maps with APIs and WebServices. Lecture Notes in Geoinformation and Cartography*; Peterson, M., Ed.; Springer: Berlin/Heidelberg, Germany, 2012; pp. 265–278.
58. Turrell, F.M. Growth of the photosynthetic area of citrus. *Bot. Gaz.* **1961**, *122*, 284–298. [[CrossRef](#)]
59. Schumann, A.W. Performance of an ultrasonic tree volume measurement system in commercial citrus groves. *Precis. Agric.* **2005**, *6*, 467–480.
60. Zaman, Q.U.; Salyani, M. Effects of foliage density and ground speed on ultrasonic measurement of citrus tree volume. *Appl. Eng. Agric.* **2004**, *20*, 173. [[CrossRef](#)]
61. O’Cuilinn, M. Wisconsin aerial photography project presents special challenges to contractors. *Earth Obs. Mag.* **1994**, *3*, 44–46.
62. Allan, A.L. A simple control system for the photogrammetric survey of a tree. *Surv. Rev.* **1998**, *34*, 373–378. [[CrossRef](#)]
63. Torres-Sánchez, J.; Lopez-Granados, F.; Serrano, N.; Arquero, O.; Peña, J.M. High-throughput 3-D monitoring of agricultural-tree plantations with unmanned aerial vehicle (UAV) technology. *PLoS ONE* **2015**, *10*, e0130479. [[CrossRef](#)]
64. Panagiotidis, D.; Abdollahnejad, A.; Surový, P.; Chiteculo, V. Determining tree height and crown diameter from high-resolution UAV imagery. *Int. J. Remote Sens.* **2017**, *38*, 2392–2410. [[CrossRef](#)]
65. Brown, P.L.; Doley, D.; Keenan, R.J. Estimating tree crown dimensions using digital analysis of vertical photographs. *Agric. For. Meteorol.* **2000**, *100*, 199–212. [[CrossRef](#)]

66. Moorthy, I.; Miller, J.R.; Berni, J.A.J.; Zarco-Tejada, P.; Hu, B.; Chen, J. Field characterization of olive (*Olea europaea* L.) tree crown architecture using terrestrial laser scanning data. *Agric. For. Meteorol.* **2011**, *151*, 204–214. [[CrossRef](#)]
67. Colaço, A.F.; Trevisan, R.G.; Molin, J.P.; Rosell-Polo, J.R. Orange tree canopy volume estimation by manual and LiDAR-based methods. *Adv. Anim. Biosci.* **2017**, *8*, 477–480. [[CrossRef](#)]



© 2020 by the authors. Licensee MDPI, Basel, Switzerland. This article is an open access article distributed under the terms and conditions of the Creative Commons Attribution (CC BY) license (<http://creativecommons.org/licenses/by/4.0/>).